https://doi.org/10.52973/rcfcv-e34481 Revista Científica, FCV-LUZ / Vol. XXXIV, rcfcv-e34481

Protective Effect of Silymarin and Mitoquinone (MitoQ) Aganist Hepatotoxicity of Cadmium Telluride Quantum Dot (CdTe QDs) Nanoparticles in Mice

Efecto protector de la silimarina y la mitoquinona (MitoQ) contra la hepatotoxicidad de las nanopartículas de puntos cuánticos de telururo de cadmio (CdTe QDs) en ratones

Seda Şimşek[1], Merve Solmaz[1], İsmail Hakkı Nur[2], Muslu Kazım Körez[3], Nejat Ünlükal[1], Ender Erdoğan[1]*

[1]*Selcuk University, School of Medicine, Department of Histology and Embryology. Konya, Türkiye.*
[2]*Erciyes University, School of Veterinary, Department of Anatomy. Kayseri, Türkiye.*
[3]*Selcuk University, School of Medicine, Department of Biostatistics. Konya, Türkiye.*
**Corresponding Author: sedaatay89@gmail.com*

ABSTRACT

As a result of the increasing use of quantum dots (QDs) and increased exposure of human beings to quantum dots, the study of the toxicity of the particles has become an important issue. In this study, the protective activity of silymarin and mitoquinone (MitoQ), which are known to have antioxidant properties, on the histopathological and biochemical changes observed in the liver of mice treated with CdTe QDs was investigated. 26 male Swiss mice were randomly divided into four groups: Control (G1), CdTe QDs (G2), silymarin + CdTe QDs (G3), mitoquinone + CdTe QDs (G4) application groups. Animals were sacrificed 24 hours (h) after injections and hyperspectral microscopy images were obtained. According to the ICP-MS results, the CdTe QDs injected through the tail vein accumulated in the liver at the end of 24 h and caused tissue damage according to the hematoxylin & eosin examination, and better preservation was observed with the antioxidant pre-treatment. The immunofluorescence results showed increased inflammation and apoptosis in the QDs group. It was observed that silymarin and mitoquinone decreased anti-MMP-9, anti-IL-10, anti-IL-1b, anti-TNF-α, and anti-caspase-9, TUNEL-positive cell ratio, liver MDA levels. There was no significant difference in serum TAS (P=0.509), TOS (P=0.588) levels, but antioxidants also increased tissue SOD and CAT levels. Antioxidants had no significant effect on anti-MT-MMP2 and anti-caspase-8 levels (P<0.001). In conclusion, it was shown that pretreatment of CdTe QD-administered mice with silymarin and mitoquinone can reduce oxidative stress in liver tissue and may have a protective effect through reduction of apoptosis and inflammation.

Key words: Antioxidant; quantum dot; mitoquinone; oxidative stress; silymarin

RESUMEN

Como consecuencia del creciente uso de puntos cuánticos (QD) y de la mayor exposición de los seres humanos a los mismos, el estudio de la toxicidad de las partículas se ha convertido en una cuestión importante. En este estudio se investigó la actividad protectora de la silimarina y la mitoquinona (MitoQ), conocidas por sus propiedades antioxidantes, sobre los cambios histopatológicos y bioquímicos observados en el hígado de ratones tratados con CdTe QDs. Se dividieron aleatoriamente 26 ratones suizos macho en cuatro grupos: Control (G1), CdTe QDs (G2), silimarina + CdTe QDs (G3), mitoquinona + CdTe QDs (G4) grupos de aplicación. Los animales fueron sacrificados 24 horas (h) después de las inyecciones y se obtuvieron imágenes de microscopía hiperespectral. Según los resultados de ICP-MS, los CdTe QDs inyectados a través de la vena de la cola se acumularon en el hígado al cabo de 24 h y causaron daños tisulares según el examen de hematoxilina y eosina, y se observó una mejor conservación con el pretratamiento antioxidante. Los resultados de la inmunofluorescencia mostraron un aumento de la inflamación y la apoptosis en el grupo de QDs. Se observó que la silimarina y la mitoquinona disminuyeron los niveles de anti-MMP-9, anti-IL-10, anti-IL-1b, anti-TNF-α y anti-caspasa-9, la proporción de células TUNEL positivas y los niveles de MDA hepáticos. No hubo diferencias significativas en los niveles séricos de TAS (P=0.509), TOS (P=0.588), pero los antioxidantes también aumentaron los niveles tisulares de SOD y CAT. Los antioxidantes no tuvieron un efecto significativo en los niveles de anti-MT-MMP2 y anti-caspasa-8 (P<0.001). En conclusión, se demostró que el pretratamiento de ratones tratados con CdTe QD con silimarina y mitoquinona, que tienen fuertes propiedades antioxidantes, puede reducir el estrés oxidativo en el tejido hepático y puede tener un efecto protector gracias a la reducción de la apoptosis y la inflamación.

Palabras clave: Antioxidante; punto cuántico; mitoquinona; estrés oxidativo; silimarina

Received: 04/07/2024 Accepted: 28/08/2024 Published: 05/12/2024

INTRODUCTION

Since the discovery of semiconductor engineered nanoparticles (NPs) various types of QDs (CdTe, CdSe, ZnS etc.) have been synthesized. These luminescent nanomaterials have shown great promise for a variety of applications, in particular in optoelectronics and biological labelling in recent years [1]. Thanks to its small dimensions, large surface areas, and unique optical, electronic, and chemical properties, it has increasing usage areas and so long-term potential damage to the environment and public health has therefore become a issue in recent years.

QDs have been shown to enter the bloodstream and ultimately accumulate in the liver and the mechanisms of potential hepatotoxicity are complex. QDs can be cytotoxic and cause cell stress. In particular, the toxicity of cadmium-based QDs is thought to be related to the leaching of free Cd^{2+} from the QDs core [1]. Some general mechanisms have been studied, such as cellular stress, mitochondrial dysfunction, immune responses, inhibition and biotransformation of various biomolecules, and most importantly, the formation of reactive metabolites that trigger this process [2]. Studies have shown that QDs also have the ability to activate macrophages and increase the expression of inflammatory factors [3]. However, a number of other studies have shown that the inhibition of the production of ROS is the only way to protect cells from the oxidative stress or DNA damage caused by QDs [4].

Silymarin, the seed extract of milk thistle, has long been used as a broad-spectrum herbal extract to protect the liver from various toxic substances and to treat liver damage, hepatitis and cirrhosis [5]. Studies to date have shown that silymarin and its flavonolignans have significant antioxidant, anti-inflammatory, and pro-apoptotic properties. It has very diverse biological and pharmacological activities with different biomolecular mechanisms [6, 7].

MitoQ is one of the most widely used antioxidants that targets the mitochondria. MitoQ is formed by the covalent attachment of ubiquinone or coenzyme Q, an endogenous antioxidant and component of the mitochondrial electron transport chain (ETC), to triphenylphosphonium (TPP^+) ions. TPP^+ is a lipophilic cation that pushes the ubiquinone moiety to the inner mitochondrial membrane with a negative electrochemical potential [8]. Mito Q has in vitro properties that prevent lipid peroxidation, reduce protein carbonylation and ROS levels and prevent apoptosis [9].

CdTe QDs are still widely used and reducing the adverse effects by using some antioxidant compounds would be clinically important. Although there are some in vitro and in vivo studies on using antioxidants to counteract nanoparticle toxicity [10, 11, 12], but there is no study on the hepatoprotective effect of silymarin and mitoquinone antioxidants against liver toxicity of CdTe QDs. Therefore, in this study, we aimed to find the pharmacological way to reduce the hepatoxicity of CdTe QDs by investigating the effects of the antioxidants silymarin and mitoquinone.

MATERIALS AND METHODS

Experimental design

The study used 26 male Swiss albino mice (*Mus musculus*), 8 weeks old. All animals were maintained according to the animal care guidelines of SÜDAM Ethics Committee at Selçuk University Experimental Medicine Application and Research Centre during the experiment.

26 male Swiss albino mice, were randomly divided into groups; Group 1 (G1): Control group {100 µL/animal physiological saline}: (n=5), Group 2 (G2): CdTe QDs {100 µL/animal, 10 $mg{\cdot}kg^{-1}$ CdTe core type (Sigma-Aldrich, USA) - COOH (carboxyl) functionalized, intravenously (iv)} group: (n=7), Group 3 (G3): Silymarin {(100 $mg{\cdot}kg^{-1}$ silymarin (Sigma-Aldrich, USA), intraperitoneally (ip), 2 hours (h) ago) + CdTe QDs (100 µL/animal, 10 $mg{\cdot}kg^{-1}$)} group: (n=7), Group 4 (G4): Mitoquinone {(5 $mg{\cdot}kg^{-1}$ MitoQ (Thermo Fisher, USA), ip, 2 h ago) + CdTe QDs (100 µL/animal, 10 $mg{\cdot}kg^{-1}$)}: (n=7). The experimental groups summarised in detail in FIG. 1.

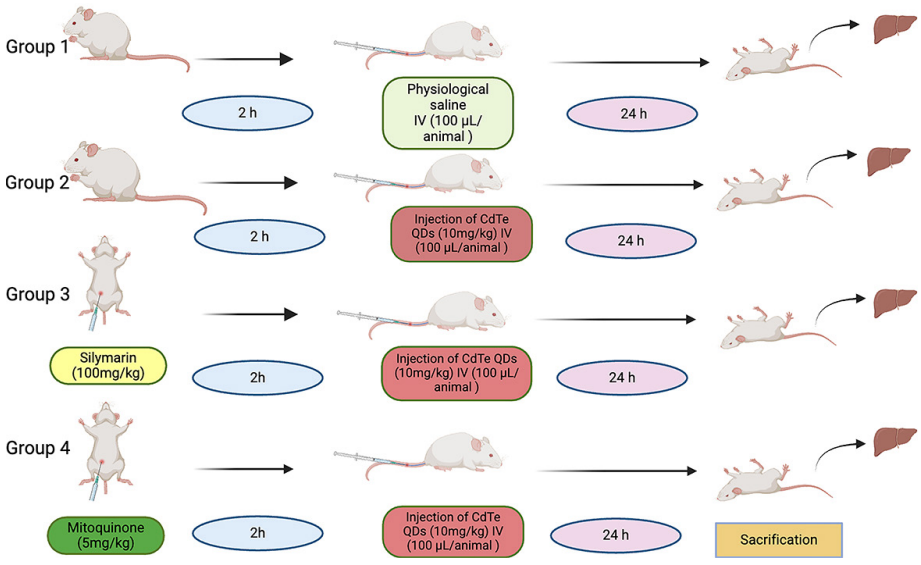

FIGURE 1. Creation of experimental groups. Group 1: Control group. Only 100 µL/animal physiological saline was administered. Group 2: CdTe QDs 10 $mg{\cdot}kg^{-1}$ dose injected into the tail vein of 100 µL/animal is the toxicity group. Group 3: 100 µL /animal at a dose of 100 $mg{\cdot}kg^{-1}$ silymarin was administered ip. After 2 hours, CdTe QDs (10 $mg{\cdot}kg^{-1}$ dose) was injected into the tail vein of 100 µL/animal. Group 4: 100 µL /animal at a dose of 5 $mg{\cdot}kg^{-1}$ mitoquinone was administered ip. After 2 hours, CdTe QDs (10 $mg{\cdot}kg^{-1}$ dose) was injected into the tail vein of 100 µL /animal. After 24 hours, the animals were sacrificed

Following a 24-hour period, the animals were anaesthetised with 60 mg·kg^{-1} ketamine hydrochloride (Ketalar®, Parke-Davis, Pfizer, Istanbul, Turkey) and 5 mg/ An ip injection of 0.6 mg·kg^{-1} xylazine hydrochloride (Rompun®, Bayer AG, Leverkusen, Germany) was administered, and in vivo hyperspectral fluorescence microscope images were obtained to visualize the overall distribution of CdTe QDs in the body following injection. Subsequently, the animals were sacrificed, and blood was collected via intracardiac puncture for the purpose of measuring total oxidant and antioxidant levels.

The liver tissues were removed without causing trauma, weighed on a precision balance, and a portion of the tissue was utilized for histological examinations, including general histopathological evaluations with H&E, immunohistochemical analysis, and anti-MT-2A for metallothionein binding to Cd+ released in the tissue . Levels of Mt-MMP2 and MMP9 antibodies and related IL10, IL-1beta and TNF alpha antibodies were measured as markers of acute inflammation. Anti-Caspases 3 and 8 levels were also measured as apoptosis markers.

An ICP-MS (inductively coupled plasma-mass spectrometry) analysis was conducted on a portion of the tissue to quantify the accumulation of Cd in the tissue. Additionally, an ELISA (enzyme-linked immunosorbent assay) analysis was performed on the remaining portion of the tissue to assess the levels of oxidative stress markers, including MDA (malondialdehyde), SOD (superoxide dismutase), and CAT (catalase).

In vivo hyperspectral fluorescent imaging

An in *vivo* imaging system (Syngene GBOX-XRQ, Cambridge, UK) was used to acquire digital images of animals in the CdTe QDs injected group under anaesthesia.

Whole body images and images of epididdymis, testis, stomach, spleen, brain, lung, heart, kidney and liver organs obtained after sacrification were taken. Imaging was performed using an epimid wave, 302 nm UV excitation and 710 nm emission filter with a scan time between 720 and 900 ms. The instrument's software program was used to process the images.

Confocal microscopy

The liver tissues of G1 and G2 fixed in 4% paraformaldehyde and embedded in cryomatrix and sections were cut at 50 μm slides using a cryostat. Confocal microscope (NIKON /Nikon A1R1, NY, USA) images of sections covered medium with DAPI (nuclear marker) (Sigma-Aldrich, MO, USA) and obtained at 10× and 40× objective magnification.

Inductively coupled plasma mass spectrometry (ICP-MS)

ICP-MS (Agilent 7500A, Tokyo, Japan) was used to analyze the quantitative measurement of the accumulation of CdTe QDs in liver, kidney, spleen, brain, heart and testis tissues after 24 h. It was performed according to the method of the Nordic Committee for Food Analysis (NMKL,186) [13]. Tissue samples were homogenised with 2 mL of 10.3 M HNO_3 at 95°C for 60 min. Samples were made up to a final volume of 5 mL with MilliQ® water. Samples were then analysed. Cumulative value was obtained by combining the organs of all animals in the G1 and G2.

Histological studies

Hematoxylin & Eosin (H&E) staining

For HE staining, tissue preparations were kept in 99.9% absolute alcohol for a few seconds and then treated with water and then kept in Harris Hematoxylin (HHS32, Sigma-Aldrich,MO, USA) [14]. After passing through water and absolute alcohol respectively, they were kept in eosin stain (HT110116, Sigma-Aldrich,MO, USA) for 1 minute. It was passed through alcohol series with increasing concentration and covered with a coverslip and entellan (1.07960, Sigma-Aldrich,MO, USA).

Immunofluorescence staining

To determine the changes in the amount of metallotheonine bound to free Cd^{+2} in the tissue, 4 μm thick liver frozen sections were labeled with polyclonal anti-MT2A primary antibody (DF6755 Affinity Biosciences, Japan). To evaluate the inflammation sections were labelled with anti-MT-MMP2 (sc-80213, Santa Cruz Biotechnology, USA), anti-MMP9 (sc-10737, Santa Cruz Biotechnology, USA), anti-TNF alpha (ABIN343428, antibodies.com, UK), conjugated anti-IL-10 (A-2) (Alexa Fluor 594, sc-365858, Santa Cruz Biotechnology, USA) and, conjugated anti IL-1 beta (Alexa Fluor 594, sc-32294, Santa Cruz Biotechnology, USA) antibodies. For the evaluation of apoptotic pathways, liver sections were labeled with anti-caspase-8 (ab4052, Abcam, United Kingdom) and anti-caspase-9 antibody (ab4053, Abcam, United Kingdom) as primary antibodies. In this immunohistochemical analysis, each section obtained from the tissue was treated individually with all these antibodies and these antibodies were marked with fluorescently labeled secondary antibodies, making the presence of these markers selected for inflammation and apoptosis visible, and at the same time, the level was determined with the appropriate program.

For this purpose, the sections were incubated with PBS containing 5% BSA and 0.2% Triton X-100 for 30 min. After incubation with protein block solution, tissues were treated with primer antibodies (1/200 to 1/500 dilutions). Tissues were stored at 4°C overnight and then treated with fluorescently labelled secondary antibody (donkey anti-rabbit IgG-FITC (sc-2090, Santa Cruz Biotechnology, USA) and covered with DAPI-containing fluorescent cover medium.

TUNEL was performed with the Andy FluorTM 488 Apoptosis Detection Kit (ABP Biosciences, MD, USA). The internucleosomal cleavage of DNA is one of the hallmarks of apoptosis. Using terminal deoxynucleotidyl transferase (TdT)-mediated dUTP nick-end labeling (TUNEL), DNA cleavage in apoptotic cells can be detected in situ in fixed cells or tissue sections. TUNEL is highly selective for the detection of apoptotic cells. It does not detect necrotic cells or cells with DNA strand breaks resulting from irradiation or drug treatment. In the TUNEL assay, the TdT enzyme is used to catalyze the addition of tagged dUTP to the 3′ ends of cleaved DNA fragments. fluorescent dye-conjugated dUTP can be used for direct detection of fragmented DNA by fluorescence microscopy. The TUNEL Andy Fluor™ 488 Apoptosis Detection Kit contains dUTP conjugated to biotin and streptavidin conjugated to bright and photostable Andy Fluor™ 488 green fluorescent dye for bright fluorescent TUNEL staining. TUNEL (+) marked cells and DAPI (+) marked cells were counted using the Image J (National Institutes of Health, Bethesda, MD, USA) program. The apoptotic index (AI) was calculated using the formula "total apoptotic cells/total cells × 100".

All immunohistochemical procedures were performed in a dark and humid environment. Examined under a fluorescence microscope (Olympus BX51 Trinocular fluorescence microscope, Hamburg, Germany). Labelled area percentages in the recorded images were calculated using the Image J program.

TAS (Total Antıoxıdant Stress), TOS (Total Oxidative Stress), OSI (Oxidative Stress Index)

TAS and TOS levels were measured using the commercially available TAS (RL0017) and TOS (RL0024) Rel Assay Diagnostics Kit (Relassay, Turkey). The automated method is based on the photometric method using the characteristic bleaching of a more stable ABTS 2,2′ –azino–bis (3–ethylbenzothiazoline–6–sulphonic acid). Results are expressed as mmol Trolox equivalent·L^{-1} [15].

The oxidising agents present in the sample oxidise the ferrous ion–o–dianisidine complex to the ferric ion. A automated colorimetric method was used to measure total oxidant status [16]. The test has been calibrated with hydrogen peroxide and results are expressed in micromolar hydrogen peroxide equivalents per litre (μmol H_2O_2 equivalent·L^{-1}).

It is calculated according to the formula OSI = [TOS (μmol H_2O_2·L^{-1}) / TAS (μmol Trolox equivalent·L^{-1})] × 100. It indicates the oxidative stress load.

Liver SOD1 (Superoxide dismutase), CAT (Catalase), and MDA (Malondialdehyde) Levels

Superoxide dismutase (Mouse SOD1 ELISA KIT, Fine Test EM0419–, China), and catalase (Mouse CAT ELISA KIT, Fine Test EM0357–, China), which are antioxidant enzymes, and malondialdehyde, which is a quantitative indicator of fatty acid oxidation (Mouse MDA ELISA KIT), Fine Test EM1723–, China) were measured using ELISA kits. These kits are based on Double antibody–Sandwich ELISA detection method. The microplate provided in these kit have been precoated with anti SOD1, CAT and MDA antibodies.

The tissue homogenates were prepared for the measurements. Residual blood was removed by washing the tissue with pre–cooled PBS buffer (0.01 M, pH=7.4). The tissue was weighed and fragmented using a homogeniser. The homogenates were centrifuged (Sorvall ST1R Plus Thermo Scientific™, MA, USA) at 5,000 G to obtain the supernatant. The total protein concentration was determined using the BCA kit (BCA Assay Kit, Thermo Scientific™, MA , USA). Appropriate dilutions were made using sample dilution buffer. The results were read in the ELISA microplate reader (Multiskan™ FC, Thermo Scientific™, MA , USA) and expressed in units appropriate for the kit.

Statistical analysis

All statistical analyses were performed using the R statistical software language, version 4.2.1 (www.r–project.org). Before analyses, normality of data was checked using Shapiro–Wilk's normality test and Q–Q plots, and homogeneity of group variances was checked using Levene's test. Results are presented as mean ± standard error.

The liver and organ weights which were weighed on an electronic digital scale (Bovoisin, U.S.A.) , MDA, SOD, CAT levels in liver, biochemical parameters and immunofluorescence staining results of the animals according to the study groups were analysed by using One–Way Analysis of Variance if the data were normal distributed and the group variances were homogeneous; Welch F (Robust ANOVA) test if the data were normal distributed but the group variances were not homogeneous; Kruskal Wallis test if the data were not normal distributed. Tukey HSD, Games–Howell test and Dunn test with FDR (false discovery rate) correction were used for multiple comparisons for the parameters that were found to be different between the groups as a result of these tests, respectively.

All results were also presented in FIGUREs using box plots. Differences between groups are indicated by '*'. The significance level was set at 5%. For FDR correction, the significance level was corrected to 0.0083.

RESULTS AND DISCUSSION

A comparison of the total weights of 26 animals before sacrifice and liver weights after sacrifice by study groups is shown in TABLE I.

According to the results obtained, the live weights of the animals were similar between all groups (*P*=0.288). After sacrifice, the liver weights of animals in the G2 group were significantly higher than those in the silymarin treatment group (G3) (adjusted *P*=0.039). In accordance with previous studies, it is thought that there is an increase in liver weight due to increased cell infiltration as an acute toxicity response [17, 18].

In Vivo Hyperspectral and Confocal Microscope Images of CdTe QDs

The distribution of CdTe QDs in the body after injection can be seen where there is an intense glow in the hyperspectral images. In the non–sacrificed animals, the distribution in the organs is not clearly visible due to their thick skin and fur, while the injection site is clearly visible from the tail vein (FIG. 2A). According to the graph of fluorescence intensity between organs, the liver, kidney and spleen accumulated more than other organs (FIGS. 2B, 2C, 2D).

Confocal microscopy was used to confirm the presence of CdTe–QDs injected through the tail vein in the liver. In the images obtained, CdTe QDs were seen in red colour with Rhodamine filter (exiemission range 690 nm–730 nm), whereas nuclei were seen in blue colour with DAPI filter (emission range 425 nm–475 nm) and the merged images of the two are shown in FIG. 2. CdTe QDs accumulated in liver cells and sinusoids.

TABLE I
Total weight of animals before sacrification and liver and kidney weights after sacrification

	Control	G2	G3	G4	*P*–value
Total weight (g)	30.40 ± 0.75	29.43 ± 0.84	31.43 ± 0.72	30.57 ± 0.37	0.288
Liver weight (mg)	1891.40 ± 104.79	1960.29 ± 46.99[b]	1605 ± 101.53[a]	1736.86 ± 59.21	0.028

[a,b] :Different small superscript letters indicate that statistically significant diffirence after multiple comparison

Detection of Cadmium (Cd^{+2}) in tissues using ICP–MS

According to cumulative evaluation of ICP–MS results, Cd^{2+} levels were highest in the spleen at the end of 24 hours, while liver and kidney reached significantly higher Cd^{2+} levels than the other tissues (FIGS. 2E, 2F, 2G). According to ICP–MS results, liver, spleen and kidney showed the highest cadmium levels, indicating that these tissues are preferential sites of CdTe–QDs accumulation [19, 20, 21, 22, 23].

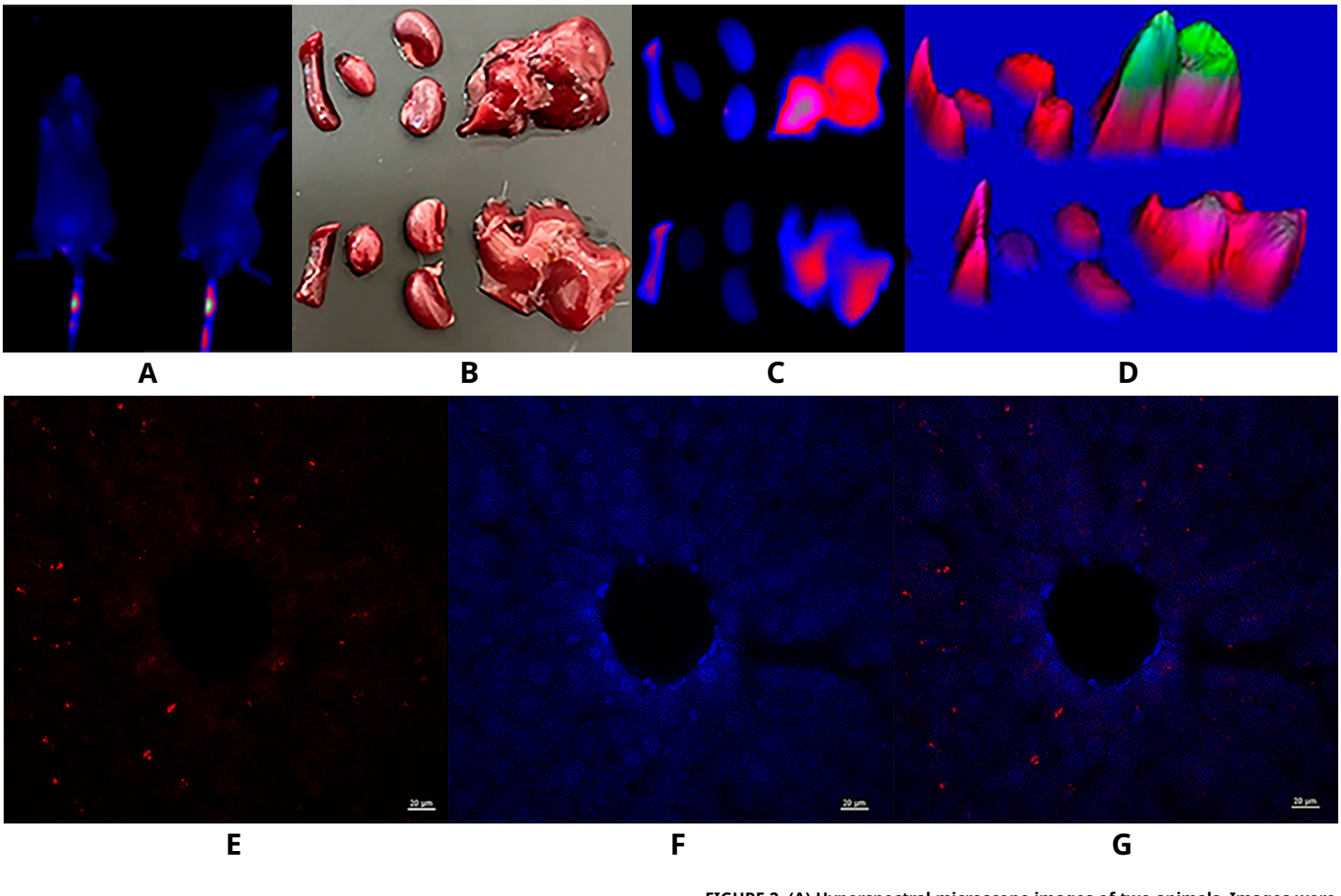

FIGURE 2. (A) Hyperspectral microscope images of two animals. Images were taken under anaesthesia. Imaging was performed using an epimid wave, 302 nm UV excitation and 710 nm emission filter with a scan time between 720 and 900 ms. (B) Spleen, heart, kidney and liver organs from left to right in two different animals after sacrification. (C) Top view of CdTe QDs density plot in organs. (D) Side view of the density plot of CdTe QDs deposited in the organs in the middle image. Colours used in the density plot; the density decreases from yellow to blue. At the end of 24 hours, images of QDs (red)(E) and nuclear dye DAPI (blue)(F) and merged images of QDs in liver tissue (G) obtained by confocal microscopy. Red coloured images were obtained with 640 nm excitation and Rhodamine emission filter (emission range 690 nm–730 nm), blue coloured nucleus images were obtained with 405 nm excitation and DAPI emission filter (emission range 425 nm–475 nm). Merged images were obtained by overlapping the two filters. Images were obtained at 40× objective magnification (scale 20 µm). (H) Results of ICP–MS measurement of Cd^{2+} accumulated in liver, kidney, spleen, heart. The results were obtained only from the animals in the CdTe QDs treated group and a cumulative evaluation was made by combining the organs from each animal. The results were given as mg Cd^{2+} per kg organ

Effects of CdTe-QDs on the morphology of the tissue

Histological sections from the liver tissues of control mice showed a normal structure. Hepatocytes were organised as cords of cells with large, globular centric nuclei, showing a smooth radial architecture around the central vein. There was no inflammatory cell infiltration or necrosis. (FIG. 3).

In G2, where CdTe QDs were applied, dilated central veins and sinusoids, congestion and loss of lobular structure, hepatocyte necrosis and occasional inflammatory cell infiltration were observed. In G3 and G4, where silymarin and mitoquinone antioxidants were applied, dilated sinusoids, binuclear hepatocytes and activated Kuppfer cells were observed. In particular, the dilated areas were less in the silymarin group than in the mitoquinone group. (FIG. 3). As mentioned earlier, congestion and inflammatory cell infiltration, which are thought to be the cause of liver weight gain, were reduced with silymarin. We believe that this result is due to the antioxidant and immunomodulatory effects of silymarin.

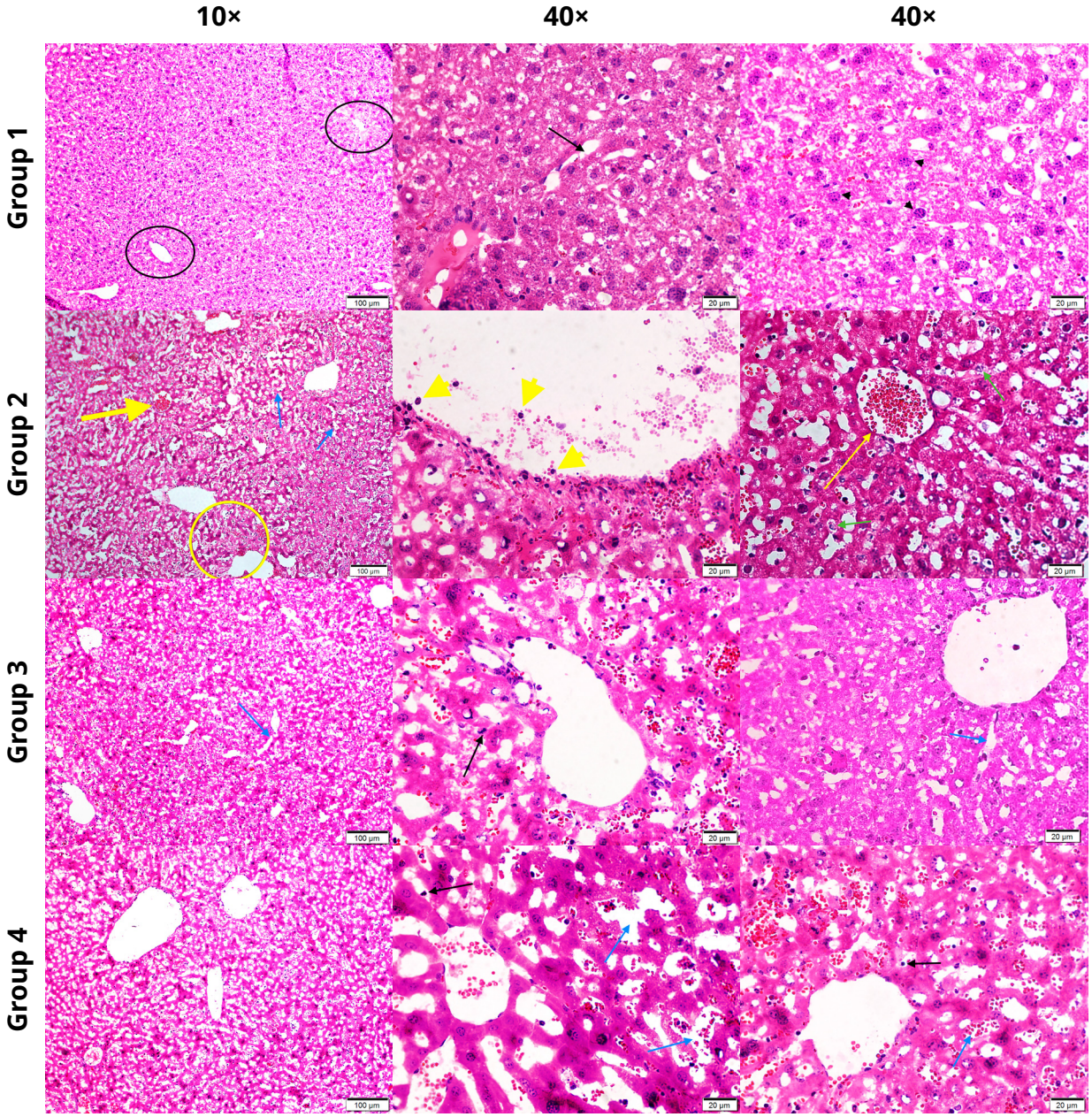

FIGURE 3. H&E images of the liver at 10× and 40× objective magnifications. Images were obtained by light microscopy. Group 1: Hepatocyte cords arranged along the central vessel (black circle), hepatic sinusoids (black arrow), hepatocytes with uniform nuclei (black arrowheads). Group 2: Loss of lobular structure (yellow circle), congestion (thick yellow arrow), inflammatory cell infiltration (yellow arrowheads), dilated sinusoids (blue arrow), hepatocyte necrosis (green arrows), dilated central vein (yellow arrow). Group 3 and Group 4: Dilated sinusoids (blue arrow), activated Kuppfer cells (fine-tipped black arrow) (Scale Bar: 10×=100 µm, 40×=20 µm)

Immunofluorescence staining results

It was shown by means of hyperspectral and confocal microscopy that CdTe QDs injected intravenously into mice accumulate in liver tissue after 24 h. CdTe QD application caused an increase in the percentage of anti-metallothionein. MT can serve as a very sensitive biomarker when the living body is exposed to Cd^{2+} stress [24] Furthermore, Lin *et al.* reported that only free Cd^{2+} dissociated from QDs, but not the QDs themselves, can induce MT production in tissues [25]. Therefore, a good biological index of QDs degradation in vivo may be the expression of an increase in MT. CdTe QD application caused an increase in the percentage of anti-metallothionein. However, metallothionein levels in the groups pre-treated with silymarin and MitoQ prior to CdTe QD application were found to be at the same level as in the group treated with CdTe QDs alone. According to this result, neither silymarin nor MitoQ had any effect on the release of Cd^{2+} from CdTe QDs. It is known that this situation is not within the mechanism of action of the selected antioxidants and that the antioxidant properties are exerted by very different mechanisms [26, 27]. The results are summarised in TABLE II.

An increase in the levels of all inflammatory response-related markers was observed in the CdTe QDs (G2) treated group compared to the control group. The increased level of anti-matrix-type metalloproteinase 2 (anti-MT-MMP2) after CdTe QD application was not affected by silymarin or mitoquinone pretreatment and was higher than in the control group. The level of anti-MMP9 was increased after CdTe QD application compared to the control group, while it was lower in the silymarin pre-treated group. The anti-MMP9 level in the mitoquinone pre-treated group (G4) was similar to that in the G2 and G3 groups (TABLE II). The percentage of fluorescent area labelled with anti-IL-10 antibody increased in the CdTe QD-treated group compared to the control group, and silymarin and mitoquinone pretreatment showed increased IL-10 levels compared to the control group, while it was observed at a similar level in the CdTe QD group (TABLE II). A significant increase in IL-1 beta levels was observed in the CdTe QD group compared to the control group. IL-1 beta levels in the silymarin pretreatment group and in the mitoquinone pretreatment group were higher than in the control group, but lower than in the CdTe QD group (TABLE II). The percentage of TNF-alpha labelled area increased with CdTe QD application and was lower in the silymarin pre-treatment group, whereas it was at the same level in the mitoquinone pre-treatment control group (TABLE II).

According to immunolabelling results of this study, the anti-MT-MMP 2, anti-MMP 9, anti-IL-1 beta, anti-TNF-a and anti-IL-10 antibodies imaged under fluorescence microscope that CdTe QDs increased inflammation. MMPs have regulatory functions in inflammation and immunity [28]. In recent years, there has been great interest in elucidating the roles of MMPs in acute liver injury. MMP-9 is an inducible gelatinase expressed by leukocytes in acutely damaged livers [29]. In a study, Si QDs administration resulted in a two – to three-fold increase in gene expression levels of matrix metalloproteinases (MMP 2 and MMP-9) [28]. According to the data obtained from studies that QDs increase the production of proinflammatory and anti-inflammatory cytokines such as IL-1β, 2, 4, 6, 8, and 18, and INF-γ, TGF-β, CRP, MIF, TNF-α, NF-kB, and CYP1A1 [21, 22, 23, 24, 25, 26, 27, 28, 29, 30, 31, 32, 33].

According to the anti-metallothionine immunolabelling results, silymarin had no protective effect on the degradation of CdTe QDs. Silymarin has been shown to significantly reduce inflammation and associated MMP-9 levels through suppression of IL-1beta and TNF-a levels. In antioxidant therapy studies, silymarin was found to reduce the expression of MMPs [6, 34, 35, 36].

It was observed that MitoQ cannot prevent the degradation of CdTe QDs. It can reduce anti-TNF α from inflammatory responses to control level in the liver and reduce anti-IL-1 beta and anti-IL-10 levels.

Confocal microscopy images of antibody labelling associated with the inflammatory response in liver tissue are shown in FIG 4.

Evaluation of Apoptosis

CdTe QDs accumulated in the liver increased the anti-caspase 8 and 9 levels. Pretreatment of silymarin and mitoquinone before the CdTe QDs could not change these levels (FIG 5A, 5B). FIGURE 5 shows a fluorescence microscopic image of liver tissue stained with anti-anti-caspase 8 and 9.

CdTe QD application significantly increased the percentage of TUNEL positive cells in the liver. Both silymarin and mitoquinone pretreatments decreased the percantage of TUNEL positive cells.

A fluorescence microscope image of the TUNEL-positive cells in the liver is shown in FIGURE 5.

It has also been found to CdTe QDs increase anti-caspase 8, which is part of the extrinsic apoptosis pathway and anti-caspase 9, which is part of the intrinsic apoptosis pathway, and apoptotic cell death (TUNEL positive cells).

Silymarin was shown to reduce apoptotic cell death (TUNEL), but not caspase-8 activation. Apoptosis has complex pathways, and it appears that silymarin could not protect the increasing extrinsic pathways of cell death markers, but it could clearly protect against DNA damage.

It has been observed that MitoQ does not significantly alter the levels of anti-caspases. However, it decreased the number of TUNEL-positive cells. During the design of the study, it was thought that the protective effect of MitoQ could be distinguished from silymarin by the change in caspase 9 levels, as it directly targets the mitochondria. This is because the main protective effect of MitoQ was to reduce the generation of oxidative stress by protecting mitochondrial integrity. However, according to the results, MitoQ did not produce a significant difference in anti-caspase 8 and 9 levels. The anti-apoptotic effect was thought to prevent DNA damage by reducing free radicals in the area.

TABLE II
Fluorescence labelled percentages of Liver anti-MT2A, MT-MMP2, MMP9, IL-10, IL-1 Beta, TNF alpha

Liver	Control	G2	G3	G4	*P*-value
Metallothionein	0.68 ± 0.22^{a}	8.20 ± 1.19^{b}	8.93 ± 1.21^{b}	9.25 ± 0.69^{b}	<0.001
MT-MMP2	3.09 ± 0.47^{a}	15.95 ± 0.61^{b}	14.60 ± 0.83^{b}	14.08 ± 0.52^{b}	<0.001
MMP 9	0.50 ± 0.16^{a}	15.95 ± 0.61^{b}	12.81 ± 0.43^{c}	14.22 ± 0.69^{bc}	<0.001
IL-10	3.92 ± 0.68^{a}	8.60 ± 1.19^{b}	6.91 ± 0.66^{b}	7.03 ± 0.61^{b}	0.012
IL-1β	0.94 ± 0.25^{a}	11.23 ± 0.75^{b}	6.59 ± 1.02^{c}	5.99 ± 0.45^{c}	<0.001
TNF α	2.12 ± 0.98^{a}	16.65 ± 1.58^{b}	7.49 ± 0.42^{c}	3.66 ± 0.57^{a}	<0.001

P-value optained using one-way ANOVA. [a,b]: Different small superscript letters indicate that statistically significant difference after multiple comparison

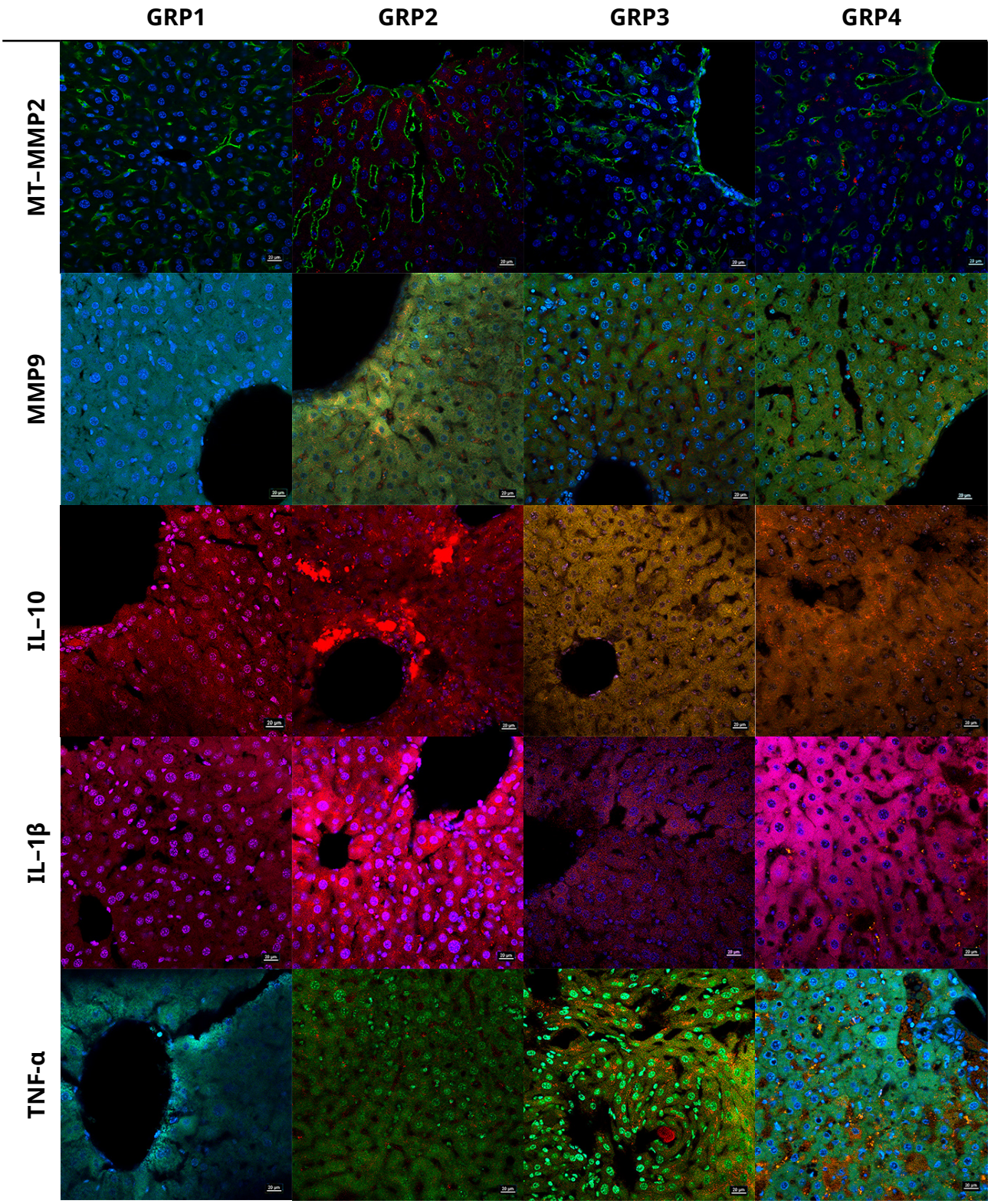

FIGURE 4. Confocal microscope images of liver MT-MMP2, MMP 9, IL-10, IL-1β, TNFα. MT-MMP2 and MMP 9 are seen in the green colour under the FITC filter (emission range 500 nm – 550 nm).TRITC filter (emission range 570nm–620nm) was used for IL-10 and coloured red in Group 1 and Group 2 and yellow in Group 3 and Group 4. For IL-1β, TRITC filter (emission range 570nm–620nm) was used and IL-1β, was coloured red and QDs were coloured yellow in Groups 1, 2 and 4 (colouring was done to avoid colour mixing due to the close emission range of conjugated antibodies and QDs for IL-10 and IL-1β,). Nuclei are seen in blue with DAPI filter (emission range 425 nm – 475 nm) and CdTe QDs with 710 nm excitation are seen in red with Rhodamine filter (emission range 650 nm – 720 nm). Sections were taken at a thickness of 50 µm. All images were obtained by superimposing these three filters. They are shown at 10× (left column) and 40× (right column) magnification (Scale 10×= 100 µm, X40= 20 µm)

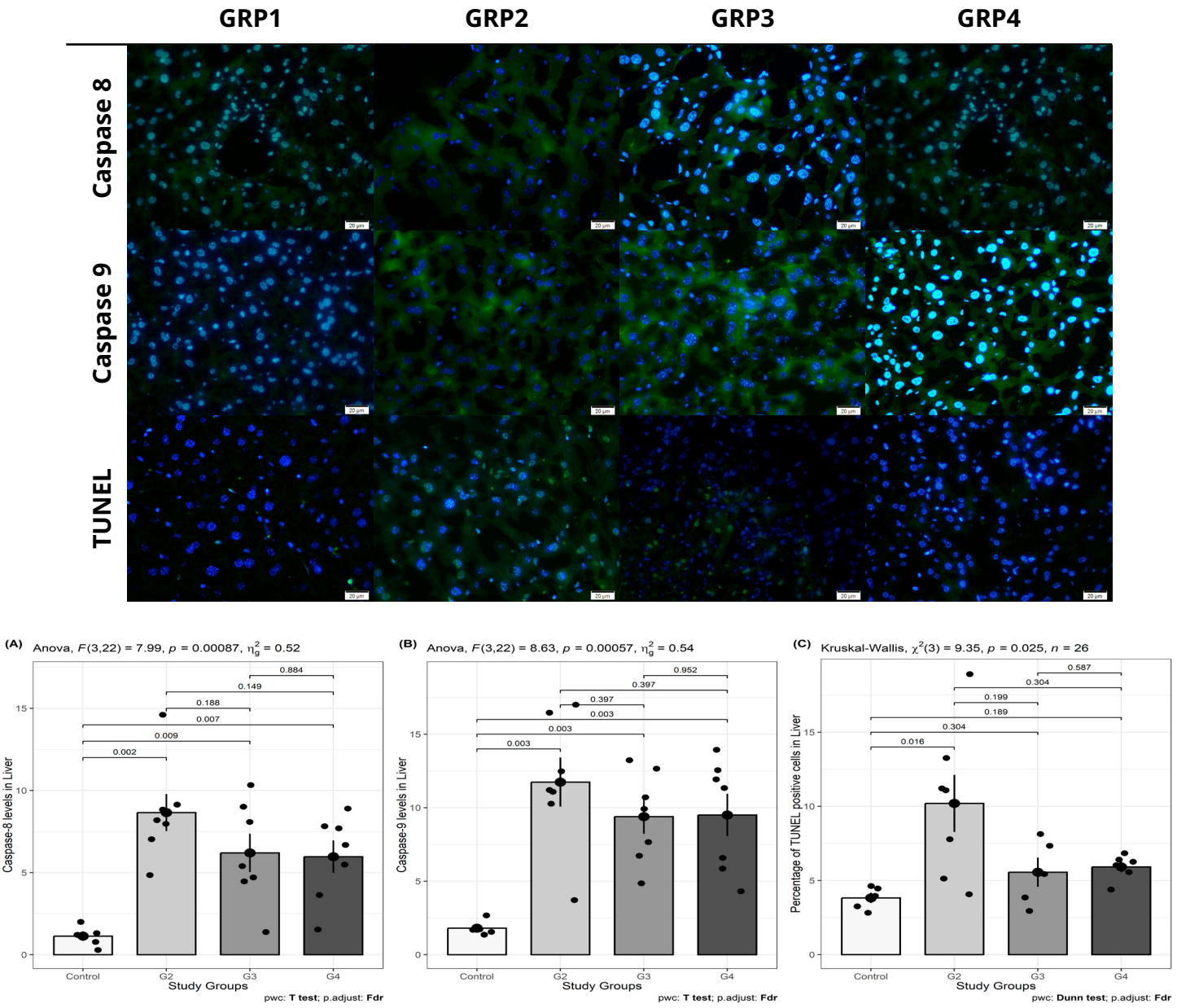

FIGURE 5. Liver Caspase 8, 9 and TUNEL fluorescence microscope images and percentage of Caspase 8, 9 and TUNEL positive cells levels. Caspase 8, 9 and the nuclei of TUNEL positive cells are seen green with FITC filter (emission range (500 nm – 550 nm) and nuclei are seen blue with DAPI filter (emission range (425 nm – 475 nm). The merged image was obtained by overlapping the two filters. Sections were taken at a thickness of 4 µm. All images were obtained at 40× magnification (Scale; 40×= 20µm). (A) Percentage of Caspase 8 antibody level and statistical differences between groups (B) Percentage of Caspase 9 antibody level and statistical differences between groups. (C) Percentage of TUNEL positive cells level and statistical differences between groups.

Effect of CdTe QDs on oxidation and antioxidation levels in serum

No significant change was observed in the oxidant and antioxidant stress parameters of CdTe application and silymarin and mitoquinone pretreatment in serum. Therefore, no significant change was observed in the oxidative stress index (OSI), which is the percentage ratio of TAS and TOS values showing the oxidative stress load (TABLE IV).

TABLE IV
TAS, TOS and OSI Results

	Control	G2	G3	G4	*P*–value
TAS	1.27 ± 0.26	1.33 ± 0.24	1.49 ± 0.60	1.60 ± 0.43	0.509
TOS	2.74 ± 1.25	4.29 ± 2.28	3.77 ± 2.30	4.06 ± 1.70	0.588
OSI	0.21 ± 0.07	0.32 ± 0.17	0.24 ± 0.10	0.26 ± 0.12	0.491

P–value optained using one–way ANOVA

Organ oxidative stress levels

CdTe QDs significantly increased the MDA level and the MDA level in the G4 was at the same level with the control group. In the G3, an increase in MDA level was observed compared to the control group (FIG. 6A). The SOD1 level of G3 and G4 was found to be higher than that of G2. The application of CdTe QDs caused an increase in SOD1 levels compared to the control group (FIG. 6B). According to the data obtained, CdTe QDs caused an increase in catalase level compared to the control group. In the G3 catalase level reached the highest value compared to the other groups. Mitoquinone pretreatment also caused an increase in catalase level compared to the control group (FIG. 6C).

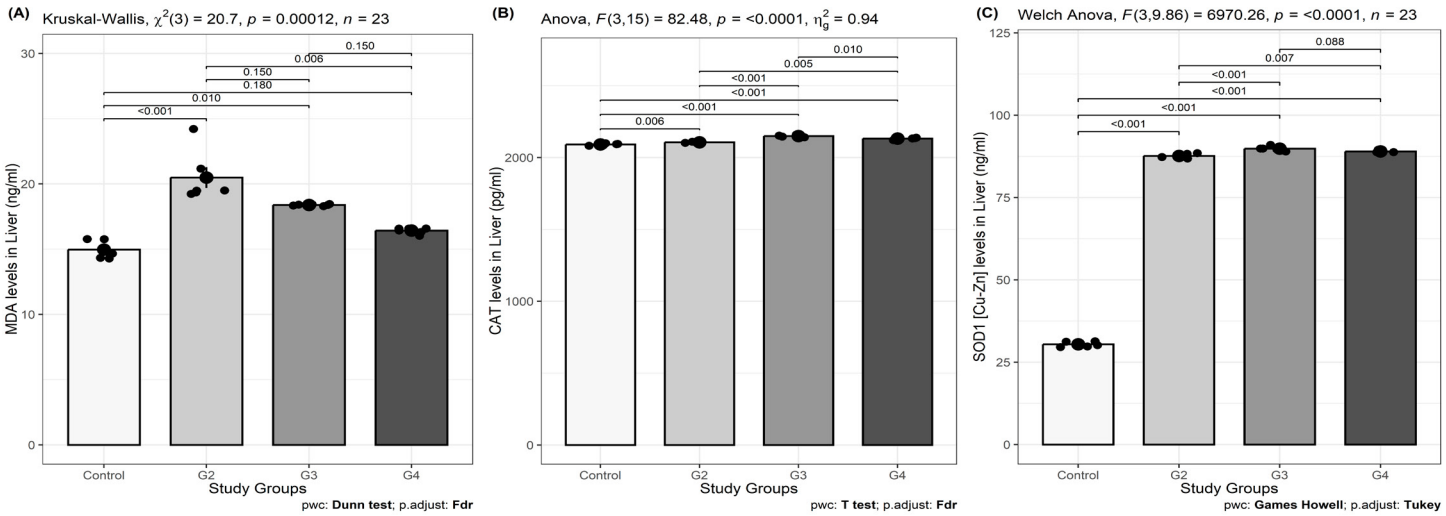

FIGURE 6. (A) Results of liver MDA and statistical differences between the groups (B) Results of liver CAT and statistical differences between the groups (C) Results of liver SOD1[Cu–Zn] and statistical differences between the groups

It was shown that TAS, TOS and OSI levels analysed in serum as markers of oxidative stress were not significantly changed. However, MDA, SOD and CAT levels analysed in liver tissue were significantly increased. According to results, although there was no change in blood oxidant and antioxidant levels, the increase in tissue oxidative stress caused by CdTe QDs was demonstrated in agreement with other studies [17, 37].

While a decrease in MDA levels was observed, tissue SOD and CAT levels increased. In their study, Negahdary *et al.* [38] observed an increase in GPX, SOD and CAT activities and a decrease in MDA levels in the group treated with silymarin and MgO NPs. In this study, an increase in malondialdehyde (MDA), superoxide dismutase (SOD) and catalase (CAT) levels was observed in the group treated with cadmium telluride (CdTe) quantum dots (QDs) nanoparticles (NPs). However, in their study, Negahdary *et al.* [38] observed a decrease in GPX, SOD and CAT activities and an increase in MDA levels in the group treated with magnesium oxide (MgO) NPs. It is hypothesised that the principal factor contributing to this discrepancy in SOD and CAT levels is associated with the variation in the dose, size, load or structure of the administered nanoparticle, in addition to the time interval between administration and analysis. It can be postulated that these toxic particles initially stimulate the activity of natural antioxidant enzymes, resulting in an increase in their concentration after 24 h. However, in prolonged applications and analyses, these particles deplete the antioxidant reserves, leading to a decline in enzyme activity [37]. Since nanoparticles have harmful effects on the body by generating ROS, this study showed that silymarin can use its antioxidant property to reduce free radicals generated by MgO NPs, as previously observed in our study [38].

In the group pre-treated with MitoQ, SOD and CAT levels increased, MitoQ prevented lipid peroxidation caused by oxidative damage in mitochondria and reduced MDA levels to control levels. It has been reported that MitoQ exerts its antioxidant effect by increasing the activation of the transcription factor Nrf2. Nrf2 upregulates the expression of antioxidant enzymes, including SOD and CAT [39]. Studies investigating the effect of mitoquinone on oxidative damage-induced SOD and CAT levels showed that MitoQ treatment significantly increased SOD and CAT mRNA levels in rats that had undergone traumatic brain injury [40]. In another study, mitoquinone treatment normalised impaired SOD and CAT expression in Sprague–Dawley rats in a common bile duct ligation (CBDL)-induced cirrhosis model [41]. It is thought that the antioxidants silymarin and mitoquinone, which we used, lowered the MDA level to a greater extent while increasing the levels of SOD and CAT, and in this way provided cellular protection.

CONCLUSION

The results of this study show that CdTe QDs accumulate in liver tissue and adversely affect it, so pretreatment with silymarin and mitoquinone reduces tissue oxidative damage, especially regulating the inflammatory response. In view of the fact that both antioxidants have effects via different pathways, it is normal that they do not have the same effect on the parameters. However, there was no apparent difference between the two of them in terms of their usefulness.

Different results in CdTe QDs toxicity studies may be dependent on various parameters such as animal species, age, sex, physical and chemical properties of the QDs used, and the route and dose of QD administration. However, in vivo studies of QDs toxicity, which are

scarce in the literature, are very valuable, and in particular studies with antioxidants will shed light on both the toxicity and the mechanism of action of antioxidants in future.

ACKNOWLEDGMENTS

The authors would like to thank SÜDAM experimental animals unit for their contribution to his study.

Financial support

This article was supported by Selcuk University Faculty Member Training Programme (ÖYP) Coordinatorship with the project number 2018-ÖYP-012.

Conflict of Interest Statement

The authors declare no conflict of interest.

BIBLIOGRAPHIC REFERENCES

[1] Yong KT, Law WC, Hu R, Ye L, Liu L, Swihart MT, Prasad PN. Nanotoxicity assessment of quantum dots: from cellular to primate studies. Chem. Soc. Rev. [Internet]. 2013; 42(3):1236–1250. doi: https://doi.org/gs9p5s

[2] Pandit A, Sachdeva T, Bafna P. Drug-induced hepatotoxicity: a review. J. Appl. Pharm. Sci. [Internet]. 2012; 2(5):233-243.doi: https://doi.org/g8tnf6

[3] Chen S, Chen Y, Chen Y, Yao Z. InP·ZnS^{-1} quantum dots cause inflammatory response in macrophages through endoplasmic reticulum stress and oxidative stress. Int. J. Nanomedicine. [Internet]. 2019; 14:9577–9586. doi: https://doi.org/g8tnf7

[4] Sharma V, Anderson D, Dhawan A. Zinc oxide nanoparticles induce oxidative DNA damage and ROS-triggered mitochondria mediated apoptosis in human liver cells (HepG2). Apoptosis [Internet]. 2012;17(8):852–870. doi: https://doi.org/f32tfs

[5] Vargas-Mendoza N, Madrigal-Santillán E, Morales-González A, Esquivel-Soto J, Esquivel-Chirino C, García-Luna YG-RM, Gayosso-de-Lucio JA, Morales-González JA. Hepatoprotective effect of silymarin. World J. Hepatol. [Internet]. 2014; 6(3):144–149. doi: https://doi.org/ggj6rw

[6] Chen IS, Chen YC, Chou CH, Chuang RF, Sheen LY, Chiu CH. Hepatoprotection of silymarin against thioacetamide-induced chronic liver fibrosis. J. Sci. Food. Agric. [Internet]. 2012; 92(7):1441–1447. doi: https://doi.org/ https://doi.org/c4s25b

[7] Zholobenko A, Modriansky M. Silymarin and its constituents in cardiac preconditioning. Fitoterapia [Internet]. 2014; 97(1):122–132. doi: https://doi.org/f6pzgb

[8] Smith RA, Porteous CM, Gane AM, Murphy MP. Delivery of bioactive molecules to mitochondria *in vivo*. Proc. Natl. Acad. Sci. USA. [Internet]. 2003; 100(9):5407-5412. doi: https://doi.org/c8rqxg

[9] Murphy MP, Smith RA. Targeting antioxidants to mitochondria by conjugation to lipophilic cations. Annu. Rev. Pharmacol. Toxicol. [Internet]. 2007; 47:629–656. doi: https://doi.org/d342dn

[10] Yan M, Zhang Y, Xu K, Fu T, Qin H, Zheng X. An *in vitro* study of vascular endothelial toxicity of CdTe quantum dots. Toxicology [Internet]. 2011; 282(3):94–103. doi: https://doi.org/cnxkz7

[11] Li X, Zhang H, Sun F. CdSe·ZnS^{-1} quantum dots exhibited nephrotoxicity through mediating oxidative damage and inflammatory response. Aging [Internet]. 2020; 13(8):12194–12206. doi: https://doi.org/g8tnf8

[12] Liu Q, Wu D, Ma Y, Cao Y, Pang Y, Tang M, Pu Y, Zhang T. Intracellular reactive oxygen species trigger mitochondrial dysfunction and apoptosis in cadmium telluride quantum dots–induced liver damage. NanoImpact [Internet]. 2022; 25:100392. doi: https://doi.org/gwkr79

[13] Julshamn K, Maage A, Norli HS, Grobecker KH, Jorhem L, Fecher P. Determination of arsenic, cadmium, mercury, and lead by inductively coupled plasma/mass spectrometry in foods after pressure digestion: NMKL interlaboratory study. J. AOAC Int. [Internet]. 2007; 90(3):844–856. doi: https://doi.org/g8tnf9

[14] Bancroft JD, Gamble M. Theory and practice of histological techniques. 6th ed. London: Churchill Livingstone; 2008. 725 p.

[15] Arnao MB, Casas JL, del Río JA, Acosta M, García-Cánovas F. An enzymatic colorimetric method for measuring naringin using 2,2'-azino-bis-(3-ethylbenzthiazoline-6-sulfonic acid)(ABTS) in the presence of peroxidase. Anal. Biochem. [Internet]. 1990; 185(2):335–338. doi: https://doi.org/dmtpgv

[16] Erel O. A new automated colorimetric method for measuring total oxidant status. Clin. Biochem. [Internet]. 2005; 38(12):1103–1111. doi: https://doi.org/dzjwc5

[17] Du Y, Zhong Y, Dong J, Qian C, Sun S, Gao L, Yan D. The effect of PEG functionalization on the *in vivo* behavior and toxicity of CdTe quantum dots. RSC Adv. [Internet]. 2019; 9(22):12218–12225. doi: https://doi.org/g8tngc

[18] Zhang T, Hu Y, Tang M, Kong L, Ying J, Wu T, Xue Y, Pu Y. Liver toxicity of cadmium telluride quantum dots (CdTe QDs) due to oxidative stress *in vitro* and *in vivo*. Int. J. Mol. Sci. [Internet]. 2015; 16(10):23279–23299. doi: https://doi.org/f7x28r

[19] Lin CH, Yang MH, Chang LW, Yang CS, Chang H, Chang WH, Tsai MH, Wang CJ, Lin P. Cd/Se/Te-based quantum dot 705 modulated redox homeostasis with hepatotoxicity in mice. Nanotoxicology [Internet]. 2011; 5(4):650–663. doi: https://doi.org/c3cbgm

[20] Su Y, Peng F, Jiang Z, Zhong Y, Lu Y, Jiang X, Huang Q, Fan C, Lee ST, He Y. *In vivo* distribution, pharmacokinetics, and toxicity of aqueous synthesized cadmium-containing quantum dots. Biomaterials [Internet]. 2011; 32(25):5855–5862. doi: https://doi.org/cdsnr7

[21] Liu J, Erogbogbo F, Yong KT, Ye L, Liu J, Hu R, Chen H, Hu Y, Yang Y, Yang J, Roy I, Karker NA, Swihart MT, Prasad PN. Assessing clinical prospects of silicon quantum dots: studies in mice and monkeys. ACS Nano [Internet]. 2013; 7(8):7303–7310. doi: https://doi.org/f48p2q

[22] Nurunnabi M, Khatun Z, Huh KM, Park SY, Lee DY, Cho KJ, Lee YK. *In vivo* biodistribution and toxicology of carboxylated graphene quantum dots. ACS Nano [Internet]. 2013;7(8):6858–6867. doi: https://doi.org/f48mz8

[23] Yaghini E, Turner H, Pilling A, Naasani I, MacRobert AJ. *In vivo* biodistribution and toxicology studies of cadmium–free indium–based quantum dot nanoparticles in a rat model. Nanomedicine [Internet]. 2018; 14(8):2644–2655. doi: https://doi.org/gjqrpm

[24] Figueira E, Branco D, Antunes SC, Gonçalves F, Freitas R. Are metallothioneins equally good biomarkers of metal and oxidative stress? Ecotoxicol. Environ. Saf. [Internet]. 2012; 84:185–190. doi: https://doi.org/f364ht

[25] Lin CH, Chang LW, Chang H, Yang MH, Yang CS, Lai WH, Chang WH, Lin P. The chemical fate of the Cd/Se/Te–based quantum dot 705 in the biological system: toxicity implications. Nanotechnology [Internet]. 2009; 20(21):215101. doi: https://doi.org/d43skd

[26] Sulaimon L, Afolab LO, Adisa RA, Ayankojo AG, Afolabi MO, Adewolu AM, Wan X. (2022). Pharmacological significance of MitoQ in ameliorating mitochondria–related diseases. Adv. Redox Res. [Internet]. 2022; 5:100037. doi: https://doi.org/g8tngd

[27] Surai PF. Silymarin as a natural antioxidant: An overview of the current evidence and perspectives. Antioxidants [Internet]. 2015; 4(1):204–247. doi: https://doi.org/gddh4t

[28] Parks WC, Wilson CL, López–Boado YS. Matrix metalloproteinases as modulators of inflammation and innate immunity. Nat. Rev. Immunol. [Internet]. 2004; 4(8):617–629. doi: https://doi.org/bdzhqv

[29] Hamada T, Fondevila C, Busuttil RW, Coito AJ. Metalloproteinase–9 deficiency protects against hepatic ischemia/reperfusion injury. Hepatology [Internet]. 2008; 47(1):186–198. doi: https://doi.org/fsmj2h

[30] Serban AI, Stanca L, Sima C, Staicu AC, Zarnescu O, Dinischiotu A. Complex responses to Si quantum dots accumulation in carp liver tissue: Beyond oxidative stress. Chem. Biol. Interact. [Internet]. 2015; 239:56–66. doi: https://doi.org/f7rqmn

[31] Chen L, Miao Y, Chen L, Jin P, Zha Y, Chai Y, Zheng F, Zhang Y, Zhou W, Zhang J, Wen L, Wang M. The role of elevated autophagy on the synaptic plasticity impairment caused by CdSe·ZnS^{-1} quantum dots. Biomaterials [Internet]. 2013; 34(38):10172–10181. doi: https://doi.org/f5j53v

[32] Dai T, Li N, Liu L, Liu Q, Zhang Y. AMP–Conjugated Quantum Dots: Low Immunotoxicity Both *In vitro* and *In vivo*. Nanoscale Res. Lett. [Internet]. 2015;10(1):434. doi: https://doi.org/f78n5d

[33] Chen T, Li L, Lin X, Yang Z, Zou W, Chen Y, Xu J, Liu D, Wang X, Lin G. *In vitro* and *In vivo* immunotoxicity of PEGylated Cd–free $CuInS_2$/ZnS quantum dots. Nanotoxicology [Internet]. 2020;14(3):372–387. doi: https://doi.org/gs9p5t

[34] Kara E, Coşkun T, Kaya Y, Yumuş O, Vatansever S, Var A. Effects of silymarin and pentoxifylline on matrix metalloproteinase–1 and –2 expression and apoptosis in experimental hepatic fibrosis. Curr. Ther. Res. Clin. Exp. [Internet]. 2008; 69(6):488–502. doi: https://doi.org/cwwn92

[35] Ramakrishnan G, Jagan S, Kamaraj S, Anandakumar P, Devaki T. Silymarin attenuated mast cell recruitment thereby decreased the expressions of matrix metalloproteinases–2 and 9 in rat liver carcinogenesis. Invest. New Drugs [Internet]. 2009;27(3):233–240. doi: https://doi.org/fgv7ts

[36] Kanawati GM, Al–Khateeb IH, Kandil YI. Arctigenin attenuates CCl_4–induced hepatotoxicity through suppressing matrix metalloproteinase–2 and oxidative stress. Egyptian Liver J. [Internet]. 2021; 11(1):1–7. doi: https://doi.org/g58728

[37] Wang J, Sun H, Meng P, Wang M, Tian M, Xiong Y, Zhang X, Huang P. Dose and time effect of CdTe quantum dots on antioxidant capacities of the liver and kidneys in mice. Int. J. Nanomed. [Internet]. 2017; 2017(12):6425–6435. doi: https://doi.org/gbv8fg

[38] Negahdary M, Ezhgi M, Ajdary M. Effects of Silymarin on oxidative stress markers in rats treated with magnesium oxide nanoparticles. Annu. Res. Rev. Biol. [Internet]. 2014; 5(3):254–261. doi: https://doi.org/g8tngf

[39] Zhou J, Wang H, Shen R, Fang J, Yang Y, Dai W, Zhu Y, Zhou M. Mitochondrial–targeted antioxidant MitoQ provides neuroprotection and reduces neuronal apoptosis in experimental traumatic brain injury possibly via the Nrf2–ARE pathway. Am. J. Transl. Res. [Internet]. 2018 [cited 24 May. 2024]; 10(6):1887–1889. Available in: https://goo.su/PK4SWh

[40] Tabet M, El–Kurdi M, Haidar MA, Nasrallah L, Reslan MA, Shear D, Shear D, Pandya JD, El–Yazbi AF, Sabra M, Mondello S, Mechref Y, Shaito A, Wang KK, El–Khoury R, Kobeissy F. Mitoquinone supplementation alleviates oxidative stress and pathologic outcomes following repetitive mild traumatic brain injury at a chronic time point. Exp. Neurol. [Internet]. 2022; 351:113987. doi: https://doi.org/gn9pbw

[41] Turkseven S, Bolognesi M, Brocca A, Pesce P, Angeli P, Di Pascoli M. Mitochondria–targeted antioxidant mitoquinone attenuates liver inflammation and fibrosis in cirrhotic rats. Am. J. Physiol. Gastrointest. Liver. Physiol. [Internet]. 2020; 318(2):G298–G304. doi: https://doi.org/g664sp